HHS Public Access

Author manuscript

J Immunol. Author manuscript; available in PMC 2017 September 01.

Published in final edited form as:

J Immunol. 2017 March 01; 198(5): 2156–2164. doi:10.4049/jimmunol.1601757.

MLKL activation triggers NLRP3-mediated processing and release of IL-1β independent of gasdermin-D

Kimberley D. Gutierrez[1], **Michael A. Davis**[1], **Brian P. Daniels**[1], **Tayla M. Olsen**[1], **Pooja Ralli-Jain**[1], **Stephen W.G. Tait**[2], **Michael Gale Jr.**[1,3], and **Andrew Oberst**[1,3,*]

[1] Dept. of Immunology, University of Washington, Seattle, WA, USA

[2] Cancer Research UK Beatson Institute, Glasgow G61 1BD, UK

[3] Center for Innate Immunity and Immune Disease, University of Washington, Seattle, WA, USA

Abstract

Necroptosis is a form of programmed cell death defined by activation of the kinase RIPK3 and its downstream effector, the pseudokinase MLKL. Activated MLKL translocates to the cell membrane and disrupts it, leading to loss of cellular ion homeostasis. Here, we use a system in which this event can be specifically triggered by a small-molecule ligand to show that MLKL activation is sufficient to induce the processing and release of bioactive IL-1β. MLKL activation triggers potassium efflux and assembly of the NLRP3 inflammasome, which is required for the processing and activity of IL-1β released during necroptosis. Notably, MLKL activation also causes cell membrane disruption, which allows efficient release of IL-1β independent of the recently described pyroptotic effector gasdermin-D. Together, our findings indicate that MLKL is an endogenous activator of the NLRP3 inflammasome, and that MLKL activation provides a mechanism for concurrent processing and release of IL-1β independent of gasdermin-D.

Introduction

In addition to the canonical cell suicide pathway of apoptosis, it is now understood that necroptosis and pyroptosis represent alternative forms of programmed cell death(1). Unlike apoptosis, pyroptosis and necroptosis are characterized by cellular swelling and rupture(2, 3). Pyroptosis is triggered by inflammasome- or PAMP-driven activation of the inflammatory caspases, caspase-1 and caspase-11. The NLRP3 inflammasome is the best-studied inflammasome and is minimally composed of NLRP3, ASC, and caspase-1. A wide array of stimuli has been shown to activate NLRP3, with disrupted ion homeostasis and potassium efflux recently proposed as a unifying stimulus. Inflammasome assembly leads to activation of caspase-1, which cleaves and activates the recently-identified cell death effector gasdermin-D (GSDMD) (4, 5). GSDMD forms pores in the cell membrane causing disruption of its integrity and triggering release of cytosolic proteins(6, 7). Concurrent with the activation of pyroptotic cell death, inflammasome-mediated activation of caspase-1 also leads to the cleavage and activation of the cytokines IL-1β and IL-18. Pyroptosis thereby

*Correspondence to: Andrew Oberst, Phone: (+1)-206-221-7316, oberst@uw.edu.

promotes inflammation through a combination of caspase-mediated processing of IL-1β and IL-18, as well as GSDMD-mediated release of these cytokines(3).

Like pyroptosis, necroptosis is a lytic cell death program. Necroptosis is defined by activation of the receptor interacting protein kinase-1 (RIPK1) and RIPK3 to form an oligomeric “necrosome,” which leads to the phosphorylation and activation of the effector pseudokinase mixed lineage kinase domain-like (MLKL)(8). Once activated, MLKL multimerizes and translocates to the cell membrane, where it triggers ion release via pore formation, leading to cell swelling and rupture(9-11). Execution of the necroptotic program has also been associated with the processing of IL-1β through diverse mechanisms(12). These include production of reactive oxygen species (ROS)(13), altered mitochondrial dynamics(14), and death-independent, RIP kinase-mediated effects(15) leading to activation of the NLRP3 inflammasome, as well as by direct processing of IL-1β by caspase-8 associated with the necrosome(16-19). Studies have also indicated that MLKL activation could promote NLRP3 inflammasome activation(16); however, this phenomenon has been difficult to characterize because experimental induction of necroptosis requires caspase inhibition, which in turn prevents NLRP3-mediated caspase-1 activation and the production of bioactive IL-1β.

To circumvent this issue we created a system by which MLKL could be directly activated independent of upstream signals. Using this system, we demonstrate that MLKL activation alone is sufficient to trigger NLRP3 inflammasome activation, caspase-1 dependent IL-1β processing, and IL-1β release. We found that MLKL-mediated membrane disruption is sufficient to trigger release of inactive pro-IL-1β upon necroptotic cell death, but that potassium efflux and components of the NLRP3 inflammasome are required to cleave IL-1β during this process. Notably, the release of bioactive IL-1β upon MLKL activation occurs independently of the pyroptotic effector gasdermin-D. MLKL activation is therefore sufficient for both the processing and release of IL-1β, in a cell-intrinsic manner. While these findings do not exclude additional connections between RIP kinase signaling and IL-1β processing, they demonstrate an inherent mechanistic link between execution of the necroptotic program, NLRP3 inflammasome activation, and IL-1β release.

Materials and Methods

Reagents and Compounds

PMA (Phorbol 12-Myristate 13-Acetate) (Sigma, St. Louis, MO, USA; P1585-1MG) was dissolved in DMSO to a concentration of 1mM and used at a concentration of 100nM. LPS-EB Ultrapure (Invivogen, San Diego, CA, USA; tlrl-3pelps) was dissolved in endotoxin free water to a concentration of 1mg/ml and used at a concentration of 1μg/ml. Doxycyclin hyclate (Sigma, D9891-5G) was dissolved in sterile water to a concentration of 2mg/ml and used at a concentration of 2ug/ml. Nigericin (Sigma, N7143-5MG) was dissolved in ethanol to a concentration of 10mM and used at a concentration of 10μM. AP1 (Clontech Laboratories, Inc., Mountain View, CA, USA; also called ‘B/B Homodimerizer,’ catalog number 635059) was dissolved in ethanol to a concentration of 100μM and used at a concentration of 100nM. KCl was made at a stock centration of 500mM and filter sterilized. Hygromycin B (Fisher Scientific, Hampton, NH, USA; BP29521MU) was dissolved in

sterile water to a concentration of 50mg/ml and filter sterilized. Puromycin dihydrochloride (Life Technologies, Grand Island, NY, USA; A1113803). Recombinant human TNF-α (PeproTech, Rocky Hill, NJ, 300-01B) was reconstituted in PBS to a concentration of 100μg/ml and used at a concentration of 100ng/ml. zVAD (SM Biochemicals, Anaheim, CA, USA; SMFMK001) was dissolved in DMSO to a concentration of 50mM and used at a concentration of 50μM. BV6 (Smac mimetic/IAP antagonist) was a kind gift from Domagoj Vucic (Genentech, Inc. San Francisco, Ca, USA). Recombinant human IL-1β (Life Technologies, PHC-0815) was reconstituted in deionized water to a concentration of 0.1mg/ml (250,000Units/ml). Anti-hIL-1β-IgG (Invivogen, mabg-hil1b-3) was reconstituted in 1ml of sterile water to a concentration of 0.1mg/ml.

CRISPR/Cas9 gene targeting

For CRISPR/Cas9 gene targeting we used a lentivirus generously provided by Dr. Daniel B. Stetson(27). The guide RNA target sites are listed below. VSV-G pseudotyped, self-inactivating lentivirus was prepared by PEI (Polysciences, Warrington, PA, USA; 23966-2) transfection of 293T cells with 1.5μg pVSV-G, 3μg psPAX-2, and 6μg CRISPR/Cas9 lentiviral vector. Lentiviral supernatants were collected 48hr post transfection and concentrated by centrifugation at 8500xg overnight at 4°C. THP-1 cells were transduced with lentivirus and selected with 1μg/ml puromycin for 5 days. Gene targeting was evaluated by restriction fragment length polymorphism (RFLP) using restriction sites that overlapped the CRISPR targeting sites, as well as Western blot for endogenous protein. Cas9 targeting sequences used were: CASP1: AAGCTGTTTATCCGTTCCAT; ASC: CGACGCCATCCTGGATGCGC; NLRP3: CTGCAAGCTGGCCAGGTACC; RIPK3: CTCGTCGGCAAAGGCGGGTT; GSDMD: CGGCCTTTGAGCGGGTAGTC.

Constructs and cell lines

MLKL-2xFV chimeric constructs, here called acMLKL, were created by cloning full length human MLKL upstream of a tetra-glycine linker followed by two $FKBP^{F36V}$ domains. These sequences were cloned into the pSLIK lentiviral vector(22) with hygromycin resistance expression. Full length human ASC fused to mCherry was cloned into the pRRL lentiviral vector (kind gift from David Rawlings, Astrakhan A., et al. 2012) downstream of an MND promoter and upstream of a T2A-Puromycin resistance cassette. Lentivirus was made as described above and used to transduce THP-1 CRISPR cell lines and selected with 800μg/ml of hygromycin for 5 days. MLKL expression was assessed by Doxycycline treatment for 24 hours followed by Western blot for FKBP and MLKL. THP-1 cells were maintained in RPMI-1640 (Fisher Scientific, SH30027FS) supplemented with 10% FCS (Sigma, 0926-500 Ml), 10mM HEPES (Fisher Scientific, SH3023701), 0.05mM 2-mercaptoethanol (Millipore, 444203-250ML), 1mM sodium pyruvate (Sigma, S2636-100ML), 29.2 g/L glutamine (Fisher Scientific, SH3003402), 10,000 U/ml penicillin and 10,000 μg/ml streptomycin (Fisher Scientific, SV30010) and grown at 37 °C in 5% CO_2.

Immunofluorescence

Anti-FKBP12 (Thermo Fisher Scientific, Waltham, MA, USA; PA1-026A) was used to stain for the presence of MLKL-2xFV after activation with Doxycycline and AP1. DAPI

(Thermo, 62248) was used to stain the nucleus. Staining was performed as previously described(28).

Cell death analysis

Cell death assays were carried out using an IncuCyte bioimaging platform as previously described(29). Briefly, 1×10^5 THP-1 cells/well were seeded in triplicate in 24-well plates and primed with PMA, and LPS or doxycycline were added as indicated. The next day cells were treated with nigericin or AP1 in the presence of 100 nM of the cell-impermeable DNA-binding fluorescent dye Sytox Green (Life Technologies, S7020). Control cells were treated with 100nM of the cell-permeable fluorescent dye Syto Green (Life Technologies, S7559), which allows quantification of the total number of cells present in order to calculate percent cell death(29). Results depicted are representative of at least three independent experiments.

Antibodies and Immunoblotting

The following antibodies were used: anti-MLKL clone 3H1(kind gift from Warren Alexander, Murphy et al., 2013), anti-RIPK3 (Novus Biologics, Littleton CO, USA; NBP2-24588), anti- Caspase-1 p10 (C-20)(Santa Cruz Biotechnology, Dallas TX, USA; sc-515), anti-actin clone C4 (Millipore, MAB1501), anti-FKBP12 (Thermo Fisher Scientific, Waltham, MA, USA; PA1-026A) anti-IL-1β (H-153)(Santa Cruz Biotechnology, sc-7884), anti-GSDMDC1 (64-y) (Santa Cruz Biotechnology, sc-81868), anti-NLRP3 (Adipogen, San Diego, CA, USA; AG-20B-0014), anti-ASC (TMS1) (MBL International, Woburn, MA, USA; D086-3). Secondary antibodies were purchased from Santa Cruz Biotechnology (mouse sc-2005, rat sc-2006 and rabbit sc-2313).

These antibodies were used for Western blotting of proteins harvested from whole-cell lysates and quantitated by BCA Protein Assay (Thermo Fisher Scientific, PI23277). Supernatants were collected from 5×10^4 THP-1 cells, 5 hours post treatment in serum free RPMI-1640 and concentrated by Amicon Ultra-0.5 Filters 3k membrane (Millipore, UFC500324). Proteins were separated using SDS-PAGE pre-cast gels (Invitrogen, Grand Island, NY, USA) by standard protocols. Detection was accomplished using ECL Western Blotting Substrate (Fisher, PI32209) and either standard autoradiography film (Pierce, Rockford, IL, USA) or an electronic luminescence detection platform (ChemiDoc XRS+ System, 170-8265, Bio-Rad, Hercules, CA, USA).

IL-1β quantification

IL-1β bioassay—HEK-blue™ IL-1β cells (Invivogen, hkb-il1r) were cultured according to manufacturers instructions. For each assay, 5×10^4 THP-1 cells were seeded in 96-well plates and primed with PMA and LPS and indicated cells were treated with Doxycycline for 24 hours. The next day cells were treated with either nigericin, or AP1 in fresh complete media. Cell supernatants were harvested 5 hours post treatment and diluted 1:10 in complete RPMI-1640. Three microliters of diluted supernatants were used to stimulate SEAP production from 5×10^4 HEK-blue™ cells seeded in 96-well plates in 200ul of complete DMEM for 24 hours. 5ul of HEK-blue™ supernatant was assessed for SEAP activity in 200ul of QUANTI-blue™ (Invivogen, rep-qb1) and incubated for two hours at 37°C. Absorbance was read at 630nM with a multi-mode microplate reader (Synergy HT; BioTek).

For each experiment three replicates for each experimental condition were assayed. Standard curve for each experiment was constructed using recombinant human IL-1β and used to calculate and report Units/ml of IL-1β. Error bars represent S.D. from the mean of a minimum of three independent wells. Statistical significance was calculated by students' t-test using GraphPad Prism software. Each result depicted is representative of at least three independent experiments.

IL-1β ELISA—ELISA was performed using the human IL-1beta ELISA Ready-SET Go! (eBioscience). For each experiment three replicates for each experimental condition were assayed. Error bars represent S.D. from the mean of a minimum of three independent wells. Statistical significance was calculated by students' t-test using GraphPad Prism software. Each result depicted is representative of at least three independent experiments.

Results

Creation and expression of ligand-activatable MLKL in human cell lines

To study the effects of MLKL activation on inflammasome formation, we created a form of MLKL that could be directly activated using a small-molecule ligand(20, 21). To do this, we fused full-length human MLKL to two $FKBP^{F36V}$ domains, to create an activatable version of MLKL that could be induced to oligomerize and thereby become activated in the presence of a dimerization drug (**Fig. 1A)**. We refer to this activatable form of MLKL as "acMLKL," and to the dimerization ligand as "AP1". Because constitutive exogenous expression of MLKL can reduce cell viability, we cloned this construct into the pSLIK tetracycline-inducible lentiviral vector(22) and expressed it in cells of the human monocyte line THP-1. We found that in these cells, addition of doxycycline led to induction of MLKL expression **(Fig. 1B and Supplemental Fig. 1A)**, and that subsequent addition of AP1 led to re-localization of MLKL-2xFV to the cell membrane, and to cell death **(Fig. 1B, C)**, consistent with MLKL-mediated membrane disruption.

To explore the activation of the NLRP3 inflammasome by this construct, we used CRISPR/Cas9 technology to delete the inflammasome effector caspase-1 in cells expressing acMLKL **(Supplemental Fig. 1B)**. We also created a similar cell line lacking the kinase RIPK3, which acts as an endogenous activator of MLKL and has been shown to be capable of inducing IL-1β cleavage through activation of caspase-8 under certain circumstances(16-19) **(Supplemental Fig. 1C)**. As expected, cells lacking caspase-1, but not those lacking RIPK3, were resistant to pyroptosis induced by the canonical NLRP3-activating stimulus of LPS priming followed by nigericin treatment **(Fig. 1D)**. Similarly, cells lacking RIPK3, but not those lacking caspase-1, were resistant to necroptosis induced by treatment with the canonical necroptosis-activating stimulus, comprised of TNF-α, a caspase inhibitor (zVAD), and SMAC mimetic (BV6) **(Fig. 1E)**. Importantly, both RIPK3-deficient and caspase-1-deficient cells underwent loss of membrane integrity and cell death with equivalent kinetics upon direct activation of acMLKL **(Fig. 1F and Supplemental Fig. 1D)**. This indicates that we are able to effectively ablate effectors of pyroptosis or necroptosis in human monocytes, and that our acMLKL construct allows induction of cell death independent of the canonical pyroptotic or necroptotic pathways.

In the course of these experiments, we noted that acMLKL-induced cell death occurred with a reduced magnitude compared to that induced by canonical pyroptotic or necroptotic stimuli. We suspected that this was due to heterogeneous expression of the acMLKL construct in our THP-1 cells, a common challenge with this cell type. Confirming this, we found that acMLKL activation caused ~25% of our THP-1 cells to die, but that surviving cells were insensitive to re-stimulation with AP1 (**Supplemental Fig. 1D**.) Nonetheless, we reasoned that the cell death response observed upon acMLKL activation was sufficient to allow us to study the effect of MLKL activation on assembly of the NLRP3 inflammasome.

MLKL activation triggers caspase-1-dependent IL-1β processing

To test the effect of MLKL activation on IL-1β processing, we primed THP-1 cells expressing acMLKL with LPS, then induced either caspase-1- or MLKL-dependent death via treatment with nigericin or AP1, respectively. Upon blotting for IL-1β in the supernatants of these cells, we found that, as expected, nigericin treatment triggered robust cleavage of IL-1β. However, MLKL activation also triggered release of cleaved IL-1β into the supernatants of cells treated with AP1 **(Fig. 2A)**. Cleaved IL-1β was absent from identically-treated THP-1 cells lacking caspase-1, indicating that the IL-1β processing observed upon MLKL activation was caspase-1 dependent. Lysates from these cells demonstrated robust accumulation of pro-IL-1β following LPS treatment, but IL-1β processing was absent in these lysates, indicating that the cleaved IL-1β that we observed in supernatants from these cells was not pre-formed in intact cells, but rather was produced during cell death **(Supplemental Fig. 1E)**.

In an effort to measure IL-1β release following MLKL activation in a more sensitive and quantitative manner, we performed ELISA analysis on supernatants from LPS-primed THP-1 cells treated with either nigericin or the MLKL activator AP1 **(Fig. 2B)**. As expected, nigericin treatment led to robust IL-1β release, which was partially blocked by deletion of caspase-1. However, ELISA analysis demonstrated equivalent IL-1β release from cells killed in an MLKL-dependent manner, irrespective of the presence of caspase-1. Notably, these results mirror the relative amounts of cell death observed in these cell lines upon nigericin treatment (partial protection upon ablation of caspase-1, **Fig. 1C**) and MLKL activation (equivalent death with or without caspase-1, **Fig. 1E**). Because ELISA analysis does not discriminate between processed and unprocessed IL-1β, we speculated that this assay was measuring release of both forms of IL-1β following cell death. We concluded that traditional ELISA analysis was not providing an accurate measure of the release of processed, bioactive IL-1β.

In order to measure the presence of processed, bioactive IL-1β produced upon MLKL activation, we used a reporter cell line responsive to human IL-1β. This cell line lacks TNF- and TLR-responsive pathways, but expresses the human IL-1 receptor along with a construct encoding the secreted embryonic alkaline phosphatase (SEAP) under the control of an NF-kB responsive promoter. IL-1β activity can thereby be quantified using a colorimetric assay for SEAP activity. We confirmed this using recombinant human IL-1β, which produced robust SEAP activity **(Supplemental Fig. 2A)**, and which was blocked by an IL-1R-antagonist antibody **(Supplemental Fig. 2B)**.

Using these reporter cells calibrated with recombinant human IL-1β, we were able to measure the bioactivity of IL-1β release from THP-1 cell lines. We found that MLKL activation in these cells led to the release of active IL-1β to a level similar to that observed upon nigericin treatment **(Fig. 2C)**. In both cases, the production of active IL-1β required caspase-1. Co-treatment of our reporter cells with THP-1 lysates and an IL-1R antagonist antibody blocked SEAP production, confirming that the observed activity resides with IL-1β **(Supplemental Fig. 2C)**. We therefore concluded that MLKL activation triggers caspase-1-dependent IL-1β processing and bioactivity. To gain kinetic insight into the production of bioactive IL-1β upon MLKL activation, we assessed the levels of IL-1β bioactivity present in the supernatants of THP-1 cells following acMLKL activation. We found that peak IL-1β activity was present in the supernatants of these cells between 4 and 6 hours after MLKL activation **(Fig. 2D)**, a timepoint that corresponds to robust induction of cell death by MLKL **(Fig. 1C)**. Notably, the observed bioactivity of IL-1β decreased at later timepoints, likely due to degradation of this cytokine in cellular supernatants. We therefore selected 5 hours after AP1 addition as a representative timepoint for the assessment of IL-1β production by these cells, and used this timepoint for subsequent analyses.

MLKL-dependent IL-1β processing requires NLRP3 and is independent of RIPK3

We hypothesized that membrane disruption caused by MLKL activated the NLRP3 inflammasome, leading to IL-1β processing by this complex. To test this idea, we created THP-1 cell lines lacking either NLRP3 or the essential adapter ASC using CRISPR/Cas9-mediated gene targeting **(Supplemental Fig. 1A-B)**. In these cells, activation of acMLKL triggered cell death with magnitude and kinetics comparable to wild-type THP-1 cells **(Fig. 3A)**, confirming that MLKL-mediated death does not depend on ASC or NLRP3. Further, these cells were resistant to cell death triggered by LPS + nigericin, consistent with a model in which nigericin-mediated potassium efflux activates the NLRP3 inflammasome, causing caspase-mediated cell death **(Fig. 3B)**. Notably, this model differs from a recent report indicating that nigericin-induced necrotic membrane rupture and cell death occur upstream of NLRP3 inflammasome activation(23).

We next used these cells, as well as THP-1 cells lacking RIPK3 (described in **Fig. 1)**, to assess the contribution of the NLRP3 inflammasome and the RIPK3 necrosome to IL-1β activation following MLKL-induced cell death. As expected, both cleaved and pro-IL-1β were found in the supernatants of THP-1 cells following treatment with LPS + nigericin, and the release of both species was abolished upon ablation of NLRP3 or ASC **(Fig. 3C)**. These findings are consistent with the idea that IL-1β is released upon cell death, since cells lacking NLRP3 or ASC fail to undergo pyroptosis upon stimulation with LPS + ATP **(Fig. 3B)**. In contrast, upon activation of MLKL in these cells, we observed that pro-IL-1β was released irrespective of the presence of ASC, NLRP3, or RIPK3 **(Fig. 3D)**. However, cleaved IL-1β was absent from the supernatants of cells lacking ASC or NLRP3 following MLKL activation. MLKL activation thus allows pro-IL-1β release via membrane disruption independent of the NLRP3 inflammasome. However, when the NLRP3 inflammasome is intact, MLKL activation also induces cleavage and activation of IL-1β during MLKL-mediated cell death.

We next confirmed the activation of IL-1β by the NLRP3 inflammasome using our reporter cell system. We found that, as expected, LPS + nigericin treatment triggered secretion of bioactive IL-1β, and that this activity required both NLRP3 and ASC **(Fig. 3E)**. MLKL activation led to a similar release of bioactive IL-1β, and this effect was also NLRP3 and ASC dependent. Neither nigericin-induced nor MLKL-induced secretion of bioactive IL-1β was altered in the absence of RIPK3 **(Fig. 3F)**. This indicates that formation of putative RIPK3-Caspase-8 complexes, which can mediate IL-1β processing in some conditions(16-18), does not contribute to IL-1β activation downstream of MLKL. Together, these data indicate that MLKL activation promotes formation of the NLRP3 inflammasome and caspase-1 mediated cleavage of IL-1β during MLKL-dependent cell death.

MLKL-dependent cell death is accompanied by assembly of ASC foci

To directly assess activation of the inflammasome in cells undergoing MLKL-dependent cell death, we utilized fluorescent microscopy to visualize formation of the ASC speck, a protein aggregate that accompanies inflammasome formation and pyroptosis. To do this, we expressed a fusion protein comprised of ASC and mCherry in acMLKL-expressing THP-1 cells, then assessed ASC speck formation using the IncuCyte Zoom fluorescent imaging platform. As expected, upon induction of NLRP3 activation with LPS + Nigericin in the presence of the cell-impermeable nuclear dye Sytox Green, we observed ASC foci associated with the Sytox-positive nuclei of pyroptotic cells **(Fig. 4A)**. Notably, when these cells were instead LPS primed, then killed by activation of acMLKL, we also observed ASC foci associated with dying cells **(Fig. 4B)**.

We next quantified the frequency with which acMLKL-dependent cell death caused observable ASC foci. As previously observed, acMLKL activation caused less cell death than LPS + nigericin. However, upon quantification we found that MLKL-dependent cell death led to observable ASC focus formation with a similar frequency to treatment with LPS + nigericin **(Fig. 4C)**. Together, these data indicate that MLKL-dependent cell death triggers ASC oligomerization and inflammasome formation with an efficiency comparable to that of canonical activators of the NLRP3 inflammasome.

MLKL-dependent activation of the NLRP3 inflammasome is triggered by potassium efflux

Potassium efflux has been proposed as a unifying mechanism of NLRP3 inflammasome activation(24), and nigericin activates this pathway by acting as a potassium ionophore. Consistent with this finding, we found that eliminating the potassium gradient across the cell membrane via addition of 40mM KCl to our culture media greatly reduced the pyroptosis-inducing effect of nigericin **(Fig. 5A)**. However, the death of THP-1 cells following MLKL activation was not affected by increased levels of KCl in culture media, indicating that MLKL-dependent cell death does not require an intact potassium gradient across the plasma membrane **(Fig. 5B)**.

We hypothesized that MLKL activation and subsequent cell membrane disruption could trigger potassium efflux, which would be necessary for NLRP3 activation. Consistent with this idea, we found that increased extracellular potassium levels greatly reduced the appearance of cleaved IL-1β in the supernatants of cells treated with nigericin or in cells

killed via MLKL activation **(Fig. 5C)**. Also consistent with this hypothesis, increased extracellular potassium eliminated the bioactivity of IL-1β released upon nigericin treatment or MLKL activation **(Fig. 5D)**. From these findings, we conclude that MLKL-mediated membrane disruption triggers potassium efflux that, while not required for MLKL-induced cell death, is necessary to trigger NLRP3 inflammasome assembly and IL-1β cleavage during MLKL-induced cell death.

MLKL activation triggers the processing and release of IL-1β independently of gasdermin-D

Gasdermin-D (GSDMD) was recently described as a key effector of pyroptosis. Cleavage of GSDMD by the inflammatory caspases leads to the formation of GSDMD pores in the plasma membrane(4, 5, 7). These pores represent an essential step in the execution of pyroptosis and secretion of bioactive IL-1β following both canonical and non-canonical inflammasome activation. Because MLKL can also disrupt the plasma membrane, we hypothesized that MLKL-dependent cell death might trigger both IL-1β processing and release independent of GSDMD. To test this idea, we deleted GSDMD from THP-1 monocytes expressing acMLKL **(Supplemental Fig. 2D-E)**. Consistent with earlier reports, these cells displayed a defect in the execution of pyroptosis following treatment with nigericin **(Fig. 6A)**. However, upon activation of MLKL, GSDMD-deficient cells died with kinetics similar to those of wild-type cells **(Fig. 6B)**.

To test the effect of MLKL activation on IL-1β secretion, we carried out bioassay analysis of the supernatants of both normal and GSDMD-deleted THP-1 cells following either treatment with LPS + nigericin on MLKL activation. We found that deletion of GSDMD led to a clear defect in secretion of bioactive IL-1β following LPS + nigericin treatment, consistent with a role for GSDMD in the canonical inflammasome-IL-1β pathway **(Fig. 6C)**. However, following MLKL activation, no such defect was observed: GSDMD-deficient cells secreted equivalent levels of bioactive IL-1β to normal THP-1 cells **(Fig. 6C)**. This indicates that MLKL-mediated membrane disruption can both activate the NLRP3 inflammasome and allow the release of processed IL-1β produced by this complex, independent of the effector GSDMD.

Discussion

Together, our findings indicate that activation of the necroptotic effector MLKL is sufficient to trigger assembly of the NLRP3 inflammasome, caspase-1 mediated IL-1β processing, and release of bioactive IL-1β. Bacterial pore-forming toxins are well-described activators of the NLRP3 inflammasome(25), and NLRP3 has been proposed as a sensor of necrotic cell death(23). Our findings are therefore consistent with the idea that MLKL acts as an endogenous toxin-like molecule and that MLKL-mediated membrane disruption and resultant necroptotic cell death triggers the same inflammasome-mediated pathway as bacterial toxin molecules. Notably, this effect is independent of GSDMD, which is required for efficient release of IL-1β during caspase-dependent pyroptosis.

Notably, while we find that MLKL activation is sufficient to cause assembly of the NLRP3 inflammasome and caspase-1-dependent processing of IL-1β, we did not observe that

MLKL activation could initiate pyroptosis. As shown in **Figs. 1F, 3A and 6B**, the kinetics and magnitude of cell death responses observed upon MLKL activation were similar irrespective of the presence of caspase-1, ASC, NLRP3 or GSDMD. Additional experiments using reduced concentrations of AP1 yielded similar results (not shown). Thus, in our experimental system, we were not able to observe a phenomenon wherein sub-lethal MLKL activation led to NLRP3-dependent execution of pyroptosis. This could be because MLKL can only induce sufficient potassium efflux to activate the NLRP3 inflammasome concurrently with complete membrane disruption; that is, NLRP3 inflammasome activation could occur after the "point of no return" of MLKL-dependent cell death. Additional studies, and a more complete understanding of the nature of MLKL-dependent membrane disruption, may clarify this point.

Several other connections between the necroptotic pathway and inflammasome activation have been reported, including RIP kinase-mediated induction of ROS(13), alterations in mitochondrial dynamics(14), and direct processing of IL-1β by caspase-8 associated with the RIPK1/RIPK3 necrosome(16-19). Our findings do not challenge the existence of these pathways; rather, they indicate that, irrespective of upstream signaling events, activation of MLKL leads to processing and activation of IL-1β. These findings may explain the recently-reported defects in NLRP3 inflammasome activation in macrophages lacking MLKL(26). Our findings indicate an inextricable link between the execution of necroptosis and the release of IL-1β, and implicate bioactive IL-1β and IL-18 as likely effectors of inflammatory responses to the necroptotic death of myeloid cells.

Supplementary Material

Refer to Web version on PubMed Central for supplementary material.

Acknowledgments

+This was work was supported by NIH grant R01 AI108685 (to AO), and by an NIAID Research Supplement to Promote Diversity in Health-Related Research (to KG).

References

1. Blander JM. A long-awaited merger of the pathways mediating host defence and programmed cell death. Nature Publishing Group. 2014; 14:601–618.
2. Vanden Berghe T, Vanlangenakker N, Parthoens E, Deckers W, Devos M, Festjens N, Guerin CJ, Brunk UT, Declercq W, Vandenabeele P. Necroptosis, necrosis and secondary necrosis converge on similar cellular disintegration features. Cell Death Differ. 2010; 17:922–930. [PubMed: 20010783]
3. Bergsbaken T, Fink SL, Cookson BT. Pyroptosis: host cell death and inflammation. Nat. Rev. Microbiol. 2009; 7:99–109. [PubMed: 19148178]
4. Kayagaki N, Stowe IB, Lee BL, O'Rourke K, Anderson K, Warming S, Cuellar T, Haley B, Roose-Girma M, Phung QT, Liu PS, Lill JR, Li H, Wu J, Kummerfeld S, Zhang J, Lee WP, Snipas SJ, Salvesen GS, Morris LX, Fitzgerald L, Zhang Y, Bertram EM, Goodnow CC, Dixit VM. Caspase-11 cleaves gasdermin D for non-canonical inflammasome signalling. Nature. 2015; 526:666–671. [PubMed: 26375259]
5. Shi J, Zhao Y, Wang K, Shi X, Wang Y, Huang H, Zhuang Y, Cai T, Wang F, Shao F. Cleavage of GSDMD by inflammatory caspases determines pyroptotic cell death. Nature. 2015

6. Liu X, Zhang Z, Ruan J, Pan Y, Magupalli VG, Wu H, Lieberman J. Inflammasome-activated gasdermin D causes pyroptosis by forming membrane pores. Nature. 2016; 535:153–158. [PubMed: 27383986]
7. Ding J, Wang K, Liu W, She Y, Sun Q, Shi J, Sun H, Wang D-C, Shao F. Pore-forming activity and structural autoinhibition of the gasdermin family. Nature. 2016; 535:111–116. [PubMed: 27281216]
8. Linkermann A, Green DR. Necroptosis. N. Engl. J. Med. 2014; 370:455–465. [PubMed: 24476434]
9. Dondelinger Y, Declercq W, Montessuit S, Roelandt R, Goncalves A, Bruggeman I, Hulpiau P, Weber K, Sehon CA, Marquis RW, Bertin J, Gough PJ, Savvides S, Martinou J-C, Bertrand MJM, Vandenabeele P. MLKL compromises plasma membrane integrity by binding to phosphatidylinositol phosphates. Cell Rep. 2014; 7:971–981. [PubMed: 24813885]
10. Cai Z, Jitkaew S, Zhao J, Chiang H-C, Choksi S, Liu J, Ward Y, Wu L-G, Liu Z-G. Plasma membrane translocation of trimerized MLKL protein is required for TNF-induced necroptosis. Nat. Cell Biol. 2014; 16:55–65. [PubMed: 24316671]
11. Wang H, Sun L, Su L, Rizo J, Liu L, Wang L-F, Wang F-S, Wang X. Mixed Lineage Kinase Domain-like Protein MLKL Causes Necrotic Membrane Disruption upon Phosphorylation by RIP3. Mol. Cell. 2014; 54:133–146. [PubMed: 24703947]
12. Vince JE, Silke J. The intersection of cell death and inflammasome activation. Cell. Mol. Life Sci. 2016:1–19.
13. Vince JE, Wong WW-L, Gentle I, Lawlor KE, Allam R, O'Reilly L, Mason K, Gross O, Ma S, Guarda G, Anderton H, Castillo R, Häcker G, Silke J, Tschopp J. Inhibitor of Apoptosis Proteins Limit RIP3 Kinase-Dependent Interleukin-1 Activation. Immunity. 2012; 36:215–227. [PubMed: 22365665]
14. Wang X, Jiang W, Yan Y, Gong T, Han J, Tian Z, Zhou R. RNA viruses promote activation of the NLRP3 inflammasome through a RIP1-RIP3-DRP1 signaling pathway. Nature Immunology. 2014
15. Kang T-B, Yang S-H, Toth B, Kovalenko A, Wallach D. Caspase-8 blocks kinase RIPK3-mediated activation of the NLRP3 inflammasome. Immunity. 2013; 38:27–40. [PubMed: 23260196]
16. Kang S, Fernandes-Alnemri T, Rogers C, Mayes L, Wang Y, Dillon C, Roback L, Kaiser W, Oberst A, Sagara J, Fitzgerald KA, Green DR, Zhang J, Mocarski ES, Alnemri ES. Caspase-8 scaffolding function and MLKL regulate NLRP3 inflammasome activation downstream of TLR3. Nat Comms. 2015; 6:7515.
17. Moriwaki K, Bertin J, Gough PJ, Chan FK-M. A RIPK3-caspase 8 complex mediates atypical pro-IL-1β processing. J. Immunol. 2015; 194:1938–1944. [PubMed: 25567679]
18. Shenderov K, Riteau N, Yip R, Mayer-Barber KD, Oland S, Hieny S, Fitzgerald P, Oberst A, Dillon CP, Green DR, Cerundolo V, Sher A. Cutting edge: Endoplasmic reticulum stress licenses macrophages to produce mature IL-1β in response to TLR4 stimulation through a caspase-8- and TRIF-dependent pathway. The Journal of Immunology. 2014; 192:2029–2033. [PubMed: 24489101]
19. Gurung P, Vande Walle L, Van Opdenbosch N, Weinlich R, Green DR, Lamkanfi M, Kanneganti T-D. FADD and caspase-8 mediate priming and activation of the canonical and noncanonical Nlrp3 inflammasomes. J. Immunol. 2014; 192:1835–1846. [PubMed: 24453255]
20. Quarato G, Guy CS, Grace CR, Llambi F, Nourse A, Rodriguez DA, Wakefield R, Frase S, Moldoveanu T, Green DR. Sequential Engagement of Distinct MLKL Phosphatidylinositol-Binding Sites Executes Necroptosis. Mol. Cell. 2016; 61:589–601. [PubMed: 26853145]
21. Rodriguez DA, Weinlich R, Brown S, Guy C, Fitzgerald P, Dillon CP, Oberst A, Quarato G, Low J, Cripps JG, Chen T, Green DR. Characterization of RIPK3-mediated phosphorylation of the activation loop of MLKL during necroptosis. Cell Death Differ. 2015
22. Shin K-J, Wall EA, Zavzavadjian JR, Santat LA, Liu J, Hwang J-I, Rebres R, Roach T, Seaman W, Simon MI, Fraser IDC. A single lentiviral vector platform for microRNA-based conditional RNA interference and coordinated transgene expression. Proc. Natl. Acad. Sci. U.S.A. 2006; 103:13759–13764. [PubMed: 16945906]
23. Cullen SP, Kearney CJ, Clancy DM, Martin SJ. Diverse Activators of the NLRP3 Inflammasome Promote IL-1β Secretion by Triggering Necrosis. Cell Rep. 2015; 11:1535–1548. [PubMed: 26027935]

24. Muñoz-Planillo R, Kuffa P, Martínez-Colón G, Smith BL, Rajendiran TM, Núñez G. K+ Efflux Is the Common Trigger of NLRP3 Inflammasome Activation by Bacterial Toxins and Particulate Matter. Immunity. 2013; 38:1142–1153. [PubMed: 23809161]

25. Mariathasan S, Weiss DS, Newton K, McBride J, O'Rourke K, Roose-Girma M, Lee WP, Weinrauch Y, Monack DM, Dixit VM. Cryopyrin activates the inflammasome in response to toxins and ATP. Nature. 2006; 440:228–232. [PubMed: 16407890]

26. Zhang X, Fan C, Zhang H, Zhao Q, Liu Y, Xu C, Xie Q, Wu X, Yu X, Zhang J, Zhang H. MLKL and FADD Are Critical for Suppressing Progressive Lymphoproliferative Disease and Activating the NLRP3 Inflammasome. Cell Rep. 2016; 16:3247–3259. [PubMed: 27498868]

27. Gray EE, Winship D, Snyder JM, Child SJ, Geballe AP, Stetson DB. The AIM2-like Receptors Are Dispensable for the Interferon Response to Intracellular DNA. Immunity. 2016; 45:255–266. [PubMed: 27496731]

28. Daniels BP, Holman DW, Cruz-Orengo L, Jujjavarapu H, Durrant DM, Klein RS. Viral pathogen-associated molecular patterns regulate blood-brain barrier integrity via competing innate cytokine signals. MBio. 2014; 5:e01476–14. [PubMed: 25161189]

29. Orozco S, Yatim N, Werner MR, Tran H, Gunja SY, Tait SWG, Albert ML, Green DR, Oberst A. RIPK1 both positively and negatively regulates RIPK3 oligomerization and necroptosis. Cell Death Differ. 2014; 21:1511–1521. [PubMed: 24902904]

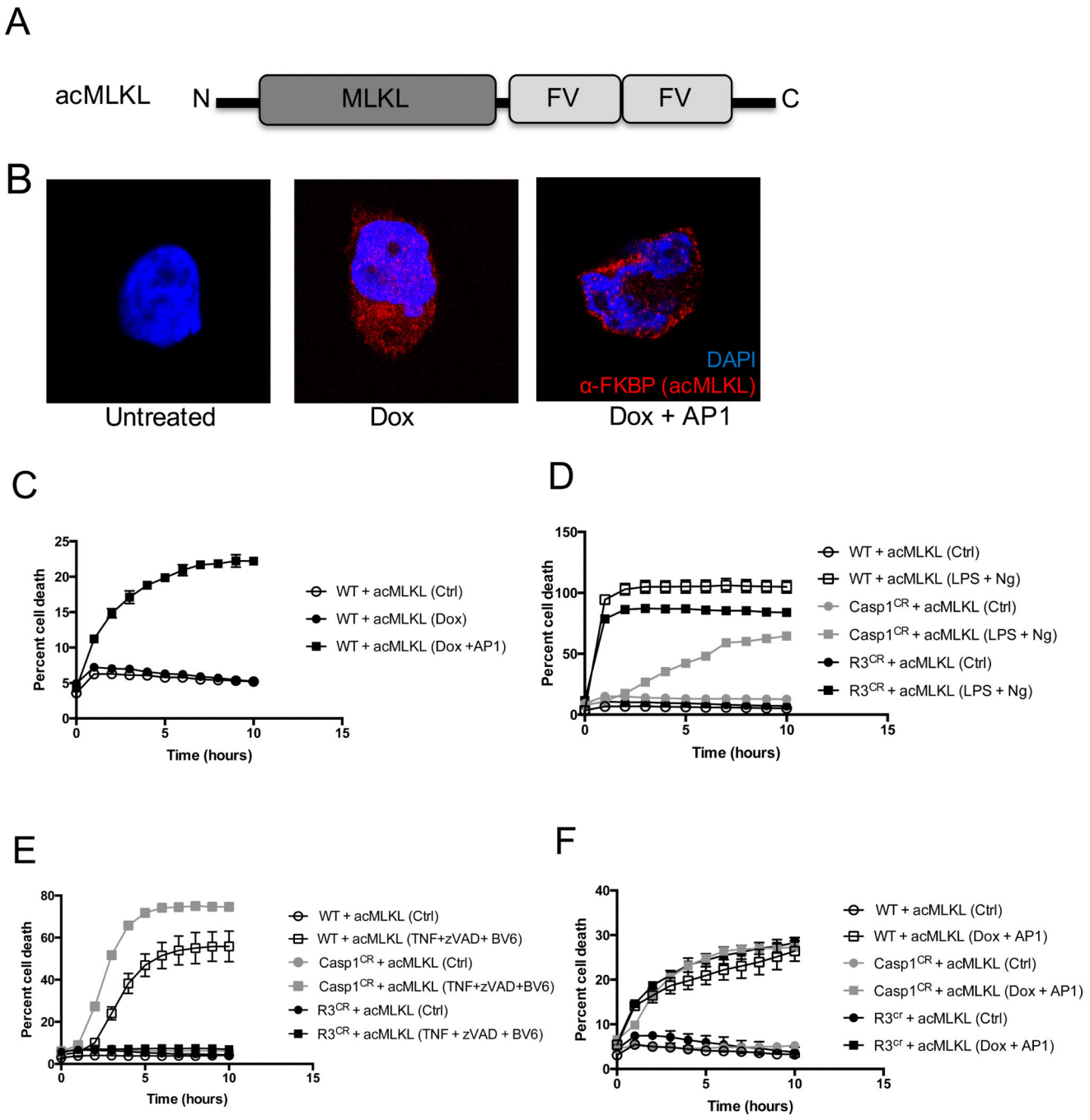

Figure 1. Direct activation of MLKL triggers cell death that is independent of caspase-1 and RIPK3

A. A schematic representation of activatable MLKL (acMLKL). **B.** Representative images of THP-1 human monocytes stably expressing acMLKL under control of a doxycycline-inducible promoter, treated as indicated then stained with DAPI (blue) and an antibody recognizing FKBP (red). Images are taken using a 63x objective with a 4x digital zoom. **C.** Cell death responses of THP-1 cells (WT) stably expressing acMLKL as in (B). "AP1" indicates the FV-binding activating ligand. **D-F.** Normal THP-1 cells (WT), or THP-1 cells

in which caspase-1 or RIPK3 expression was ablated by CRISPR targeting (Casp1^{CR} and R3^{CR} respectively) expressing acMLKL were treated as indicated. Cell death was quantified by IncuCyte bioimager. “Ng” indicates nigericin treatment. For each experiment, three replicates for each experimental condition were assayed. Error bars represent S.D. from the mean of a minimum of three independent wells.

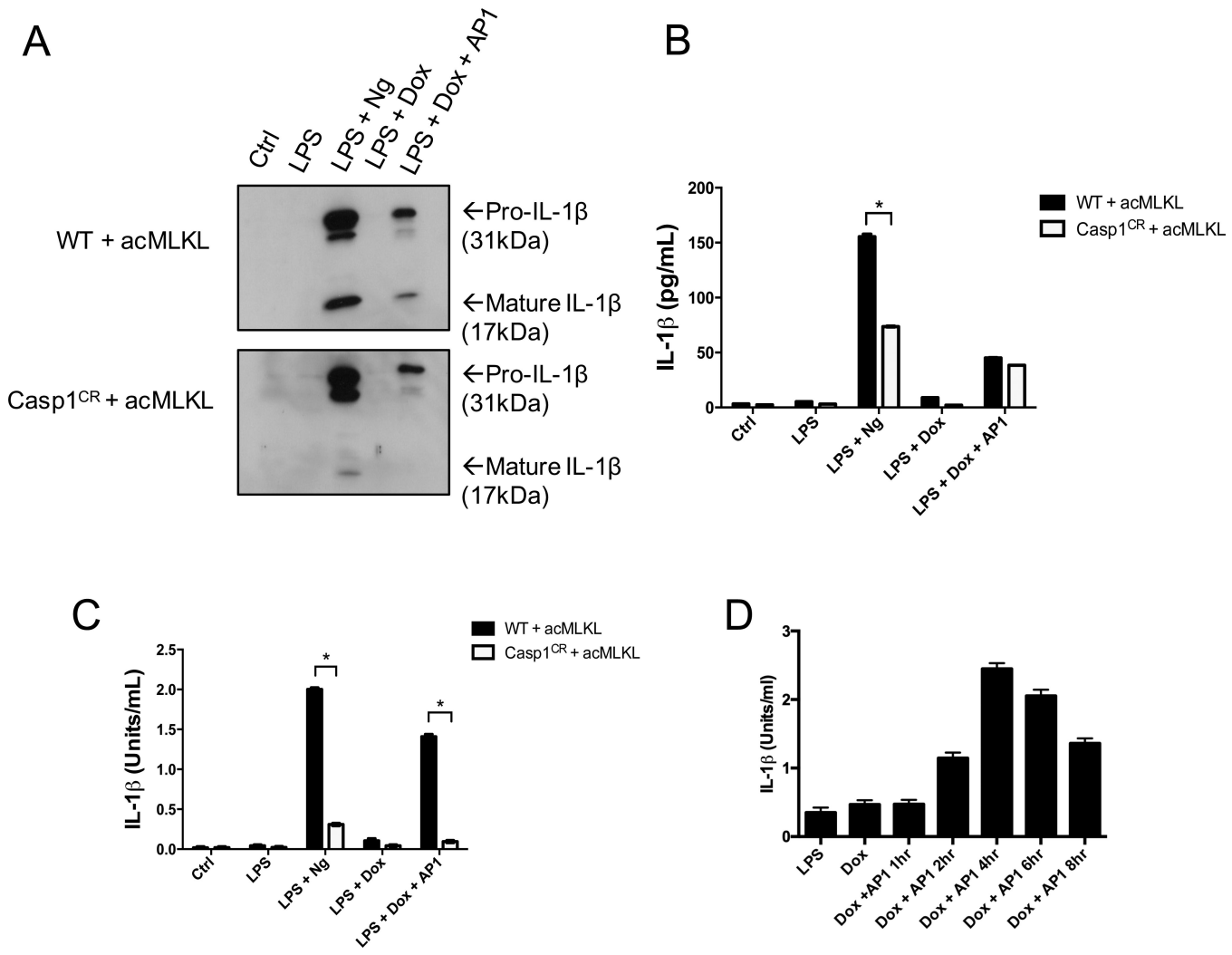

Figure 2. MLKL activation induces the release of bioactive IL-1β in a Caspase 1 dependent manner

WT and Caspase 1 CRISPR edited THP-1 cells expressing doxycycline-inducible acMLKL were treated as indicated. Supernatants were harvested 5 hours after AP1 or nigericin (Ng) treatment and IL-1β was detected or quantified by three different assays. **A.** Western blot using an antibody against human IL-1β to detect the pro- and mature forms of IL-1β. **B.** ELISA, which detects both pro- and mature forms of IL-1β, and reported as (pg/ml). **C.** IL-1β Bioassay exclusively detects the mature, bioactive form of IL-1β and is reported as (Units/ml). **D.** THP-1 cells expressing acMLKL were LPS primed and treated with doxycycline overnight, then treated with AP1. Supernatants were recovered at indicated timepoints following AP1 treatment, and IL-1β bioactivity was measured. For each experiment three replicates for each experimental condition were assayed. Standard curve for each experiment was constructed using recombinant human IL-1β and used to calculate and report international units (U)/ml of IL-1β. Error bars represent S.D. from the mean of a minimum of three independent wells. Statistical significance was calculated by student's t-test using GraphPad Prism software. Each result depicted is representative of at least three independent experiments. *$p < 0.05$

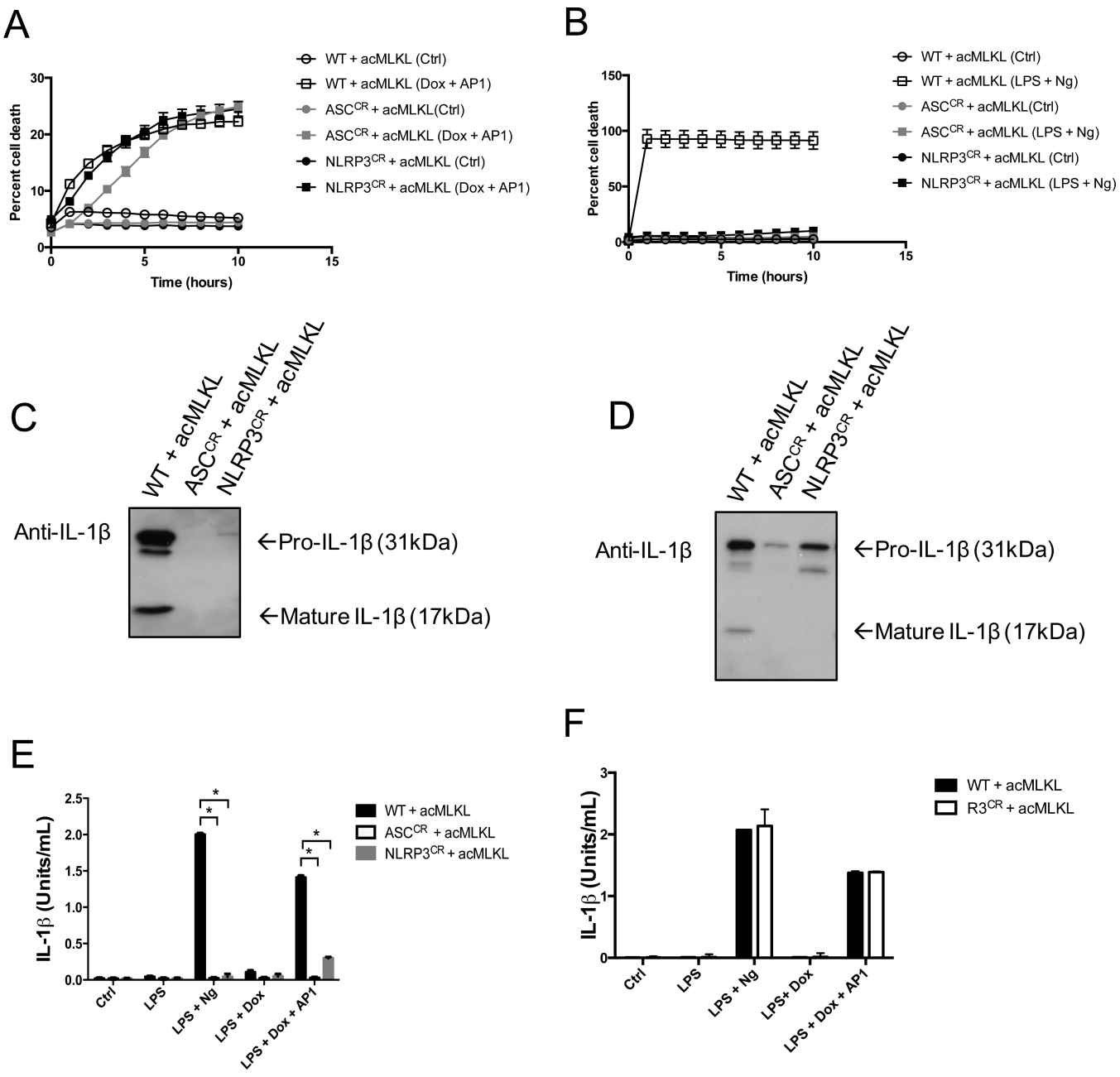

Figure 3. The NLRP3 inflammasome is required for the production of bioactive IL-1β following MLKL activation

A-B. THP-1 cells (WT) or THP-1 cells in which ASC or NLRP3 were deleted using CRISPR gene targeting (ASC^{CR} or NLRP3^{CR} respectively) stably expressing doxycycline-inducible acMLKL were created. Cell death kinetics were measured in these cells upon MLKL activation **(A)** or LPS + nigericin treatment **(B)** using an IncuCyte bioimager. **C-D.** Supernatants from these cells were analyzed by Western blotting for IL-1β following treatment with LPS + nigericin **(C)** or LPS priming followed by treatment with AP1 to activate MLKL **(D)**. **E.** IL-1β Bioassay of WT, ASC^{CR} and NLRP3^{CR} CRISPR edited cells expressing acMLKL treated as indicated. **F.** IL-1β bioassay of WT and RIPK3^{CR} cells

treated as indicated. Bioactive IL-1β in cellular supernatants was measured five hours post treatment and reported as U/ml. For each experiment three replicates for each experimental condition were assayed. Standard curve for each experiment was constructed using recombinant human IL-1β and used to calculate and report U/ml of IL-1β. Error bars represent S.D. from the mean of a minimum of three independent wells. Statistical significance was calculated by student's t-test using GraphPad Prism software. Each result depicted is representative of at least three independent experiments. *$p < 0.05$

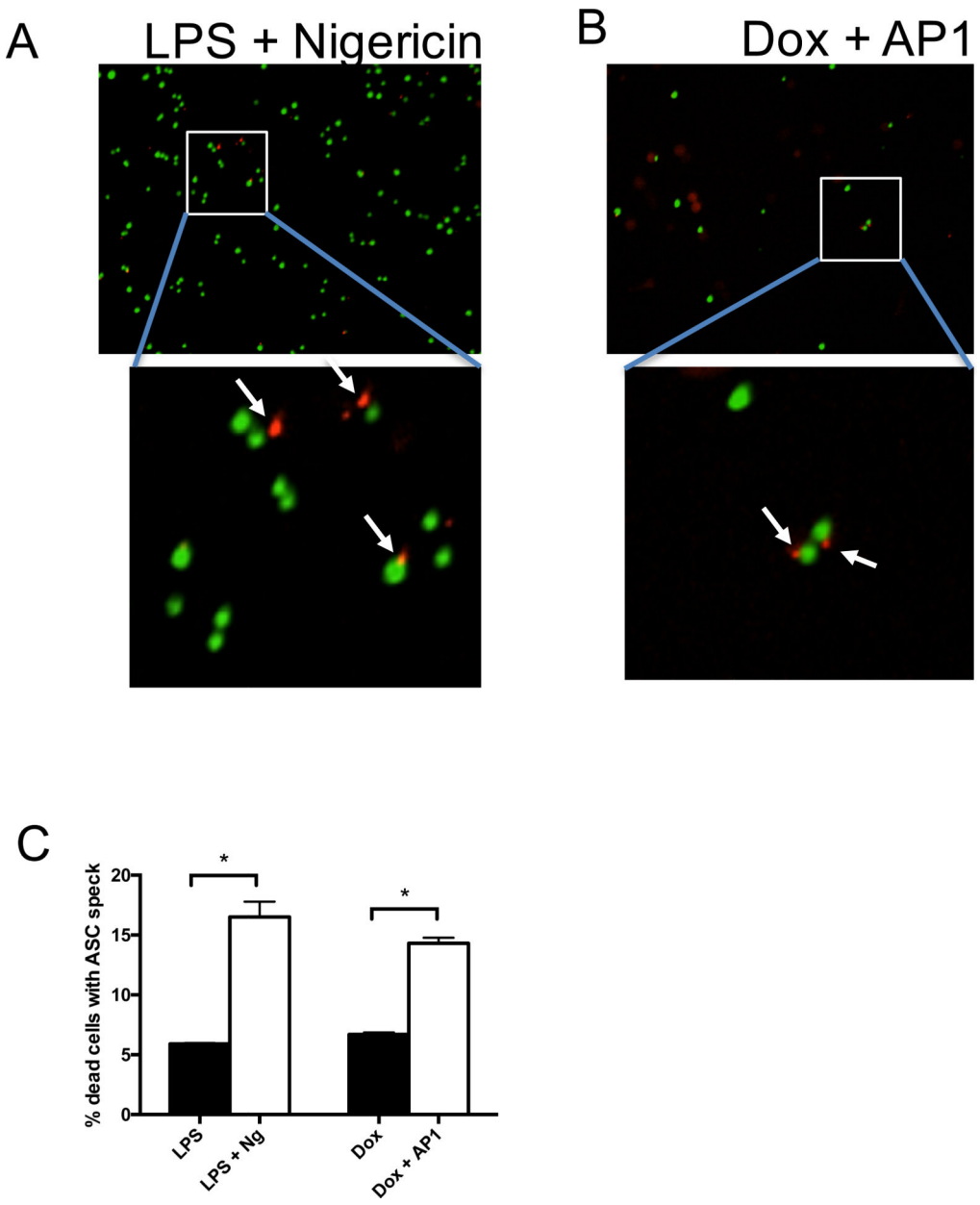

Figure 4. MLKL activation causes formation of ASC foci

THP-1 cells expressing acMLKL were stably transduced with a fusion protein comprised of ASC fused to mCherry. Cell death was induced using LPS + nigericin **(A)** or doxycycline + AP1 **(B)** in the presence of the fluorescent nuclear dye Sytox Green. Representative images were captured using an IncuCyte Zoom fluorescent imaging platform. White arrows indicated ASC foci associated with Sytox-labeled nuclei. **C.** Ten fields of cells treated as in A and B were counted by researchers blinded to the experimental treatments, and the frequency with which ASC foci were observed associated with Sytox-positive nuclei was quantified. Error bars represent S.D. from the mean of a minimum of three independent wells. Statistical significance was calculated by student's t-test using GraphPad Prism software. $*p < 0.05$

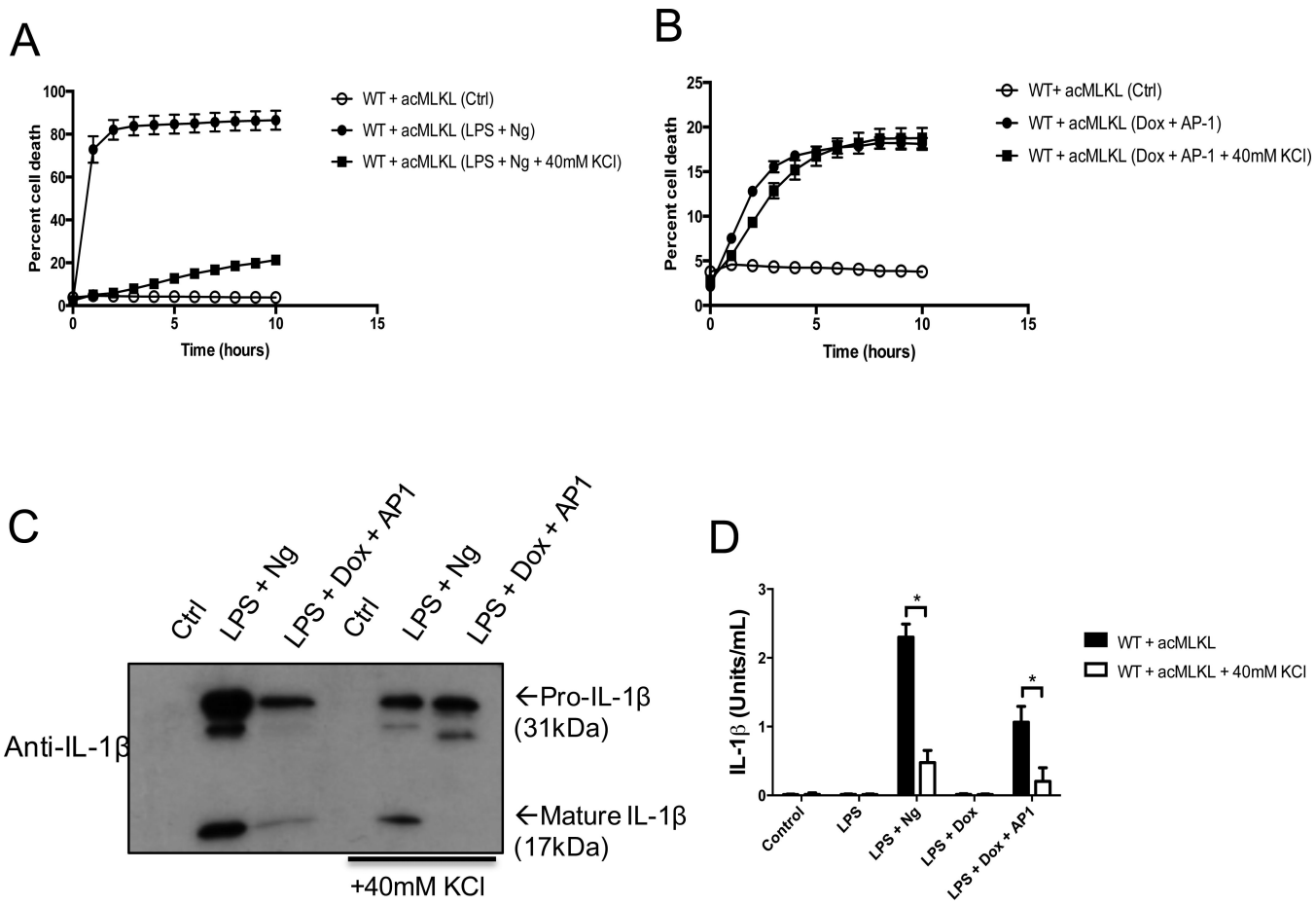

Figure 5. Potassium efflux is required for the release of bioactive IL-1β but not for cell death upon MLKL activation

A-B. Cell death kinetics of THP-1 cells stably expressing acMLKL in response to LPS + nigericin **(A)** or MLKL activation **(B)** were tracked using an IncuCyte bioimager**. C.** Western blot analysis of THP-1 cell supernatants harvested five hours after addition of nigericin or AP1. **D.** IL-1β bioassay of THP-1 cells expressing acMLKL, treated as indicated. Bioactive IL-1β in the supernatants was measured five hours post treatment and reported as (Units/ml). For each experiment three replicates for each experimental condition were assayed. Standard curve for each experiment was constructed using recombinant human IL-1β and used to calculate and report Units/ml of IL-1β. Error bars represent S.D. from the mean of a minimum of three independent wells. Statistical significance was calculated by student's t-test using GraphPad Prism software. Each result depicted is representative of at least three independent experiments. *$p < 0.05$

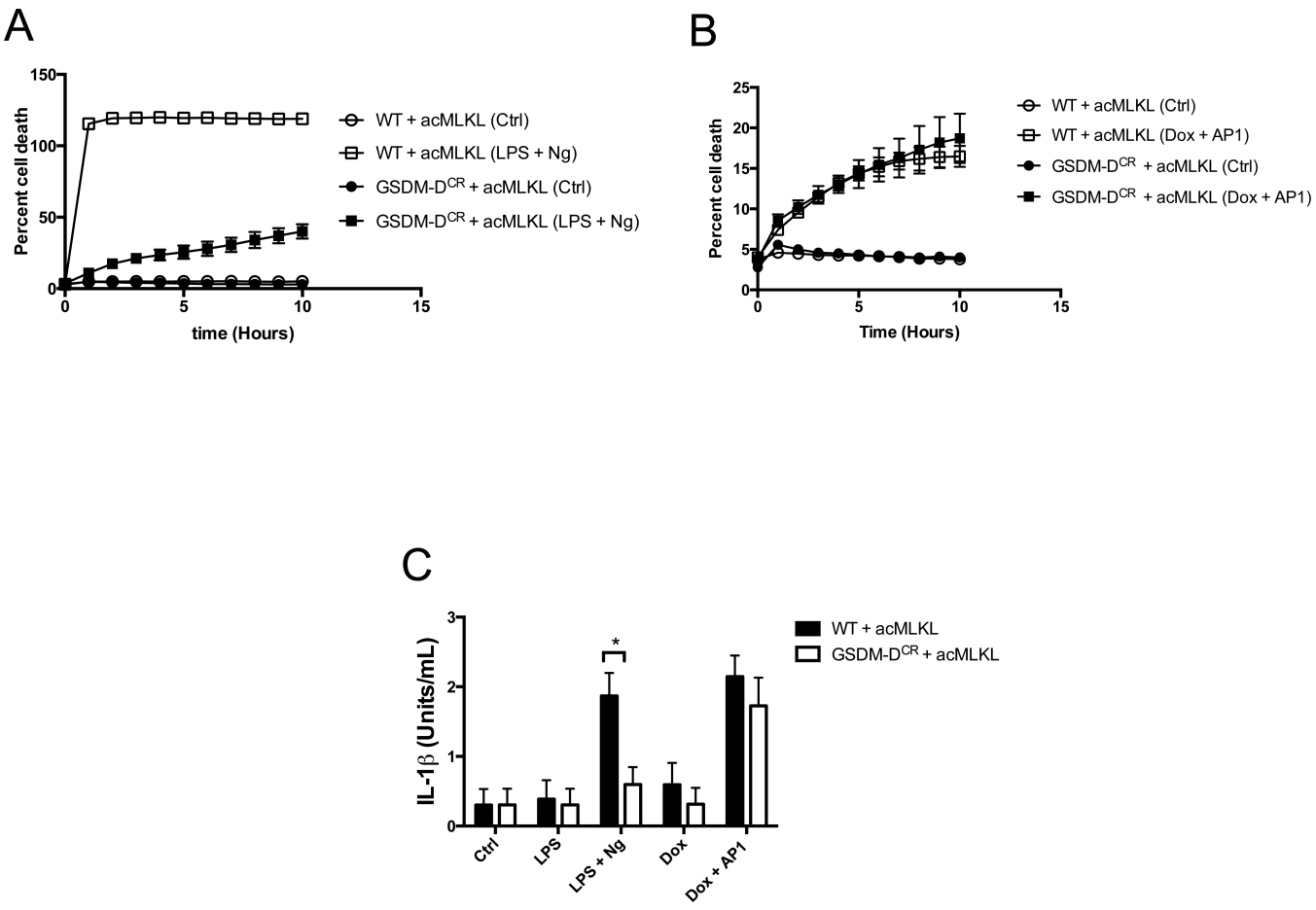

Figure 6. IL-1β production by MLKL activation is independent of Gasdermin-D

A-B. THP-1 cells (WT) or THP-1 cells in which GSDMD was deleted by CRISPR (GSDMD^{CR}) transduced with doxycycline-inducible acMLKL were treated as indicated, and cell death was tracked using an IncuCyte bioimager. **C.** IL-1β bioassay of WT and GSDMD^{CR} CRISPR cells expressing acMLKL, treated as indicated. Bioactive IL-1β in the supernatants was measured five hours post treatment and reported as (Units/ml). For each experiment three replicates for each experimental condition were assayed. Standard curve for each experiment was constructed using recombinant human IL-1β and used to calculate and report Units/ml of IL-1β. Error bars represent S.D. from the mean of a minimum of three independent wells. Statistical significance was calculated by student's t-test using GraphPad Prism software. Each result depicted is representative of at least three independent experiments. *$p < 0.05$